Resource Block-Based Co-Design of Trajectory and Communication in UAV-Assisted Data Collection Networks

Yanyan Guo, Ge Xu, Zhicai Zhang, *Member, IEEE*, Zengbiao Li, Xinzhe You, Guixia Kang, Lin Cai, *Fellow, IEEE*, and Laurence T. Yang, *Fellow, IEEE*

***Abstract*— This paper explores the joint optimization problem for trajectory planning and radio resource allocation in unmanned aerial vehicle (UAV) communications with the aim of maximizing data collection. Rather than decomposing the problem into subproblems, as most current approaches do, we express the quantity of data gathered by a UAV-assisted network as a function of both the size of the resource block allocated to all ground devices and their average upload rate. Based on this formula, it can be concluded that the problem of maximizing the average data collection can be reduced to minimizing the flight trajectory if each device communicates with the UAV within the maximum allowable coverage of the UAV. To address this issue, we propose an advanced hierarchical clustering algorithm that divides larger network-scale scenarios into many disjoint subregions to determine the initial hovering positions of the UAV. The non-convex minimization trajectory problem is decomposed into a series of convex optimizations to minimize path segments along the trajectory, based on the traveling salesman problem (TSP). Subsequently, the communication optimization process is modified to assign specific upload times for each device. The effectiveness of the optimization algorithm is demonstrated through extensive simulations, which show its superior performance in terms of average rates of data collection and upload failures.**

Manuscript received 10 April 2024; revised 23 July 2024; accepted 19 August 2024. This work was supported in part by the National Key Research and Development Program of China under Grant 2022ZD0118300 and in part by the Fundamental Research Program of Shanxi Province under Grant 202103021224024 and Grant 202103021223021. The Associate Editor for this article was J. Blum. *(Corresponding author: Zhicai Zhang.)*

Yanyan Guo, Ge Xu, Zengbiao Li, and Xinzhe You are with the College of Physics and Electronic Engineering, Shanxi University, Taiyuan 030004, China (e-mail: guoyanyan@sxu.edu.cn; 202222617053@email.sxu.edu.cn; 20200110201009@email.sxu.edu.cn; 202322615014@email.sxu.edu.cn).

Zhicai Zhang is with the School of Computer Science and Technology, Hainan University, Haikou 570228, China, and also with the School of Physics and Electronic Engineering, Shanxi University, Taiyuan 030004, China (e-mail: zzcai@hainanu.edu.cn).

Guixia Kang is with the School of Information and Communication Engineering, Beijing University of Posts and Telecommunications, Beijing 100876, China (e-mail: gxkang@bupt.edu.cn).

Lin Cai is with the Department of Electrical and Computer Engineering, University of Victoria, Victoria, BC V8P 5C2, Canada (e-mail: cai@ece.uvic.ca).

Laurence T. Yang is with the School of Computer Science and Technology, Hainan University, Haikou 570228, China, also with the School of Computer Science and Technology, Huazhong University of Science and Technology, Wuhan 430074, China, and also with the Department of Computer Science, St. Francis Xavier University, Antigonish, NS B2G 2W5, Canada (e-mail: ltyang@ieee.org).

Digital Object Identifier 10.1109/TITS.2024.3450538

***Index Terms*— Traveling salesman problem (TSP), successive convex approximation (SCA), UAV, space-air-ground-aqua integrated network (SAGAIN).**

I. Introduction

THE Internet of Things (IoT), which connects every object on the planet through a seamless network, enables everything to be intelligent and monitored through information exchange and communication [1]. In order to achieve the ambitious vision, it is necessary to implement a significant number of network-connected devices (including wearables, embedded sensors, traffic lights and street lights, connected vehicles, cameras, etc.) across a diverse range of verticals (such as healthcare, transportation, agriculture, and industry). In these applications, a substantial number of IoT devices are distributed for the purpose of sustainable monitoring in remote and inhospitable environments, including rural farmlands, forests, and disaster-stricken areas. However, the existing terrestrial networks are constrained in their coverage and are thus unable to provide the requisite network services in these locations. In order to extend human communication activities to a larger area, the space-air-ground-aqua integrated network (SAGAIN) [1] has emerged as a new and attractive research topic in the last decade, which realizes the seamless integration of air networks, satellite systems, and ground communications. As one of the most prominent components of the SAGAIN, unmanned aerial vehicle (UAV)-assisted communications can quickly provide wireless connectivity for mobile devices that are beyond the reach of terrestrial communication infrastructure. In addition, UAVs can move flexibly for line-of-sight (LoS) communications and act as a collection unit to gather information from a variety of ground devices, providing higher throughput, low latency and power savings for mobile devices with limited capabilities. UAV-assisted networks have been utilized in various applications, such as aerial inspection, precision farming, traffic management, and package delivery [2], [3].

Since UAVs are agile, flexible and mobile, the flight trajectory design needs to be more explicit about the communication performance. This performance is dependent on the user communication planning and the resource allocation given the UAV flight path [2]. Most current approaches to solving the co-design of trajectory and communication are to decompose the joint optimization into independent subproblems [2], e.g., to solve the subproblems of communication scheduling and trajectory optimization iteratively. However, it remains unclear

whether priority should be assigned to optimizing the communication link or the UAV flight path. For instance, Guo, et. al. in [3] aimed at maximizing the minimum (average) achieved rate of all terrestrial devices under the constraints of the UAVs' trajectories and communication schedules. On the other hand, in [4], Samir, et. al. focused on minimizing the UAV's flight distance while serving time-constrained data collection devices. In fact, to enhance the quality of the communication link, a UAV trajectory design necessarily requires a sufficient path that allows the UAV to approach its served equipment. Note that for any given UAV flight time, the longer the UAV flight distance, the less time the UAV has to enjoy the communication link [4], and vice versa. Another major research challenge is to optimize the flight path of UAVs. Since the trajectory depends on a large number of factors, the complexity of the optimization is prohibitive. On one hand, to simplify the optimization algorithm, many optimization schemes [3], [5] have arbitrarily determined the number of hovering positions based on specific preconditions, such as the number of devices, load balance, etc. In fact, even a one-point difference in the number of designable hovering positions can result in completely different UAV flight trajectories utilizing successive convex approximation (SCA) approach [3], [4]. Therefore, we should carefully consider this issue when optimizing UAV trajectories. On the other hand, solving non-convex optimization problems using SCA methods becomes increasingly complex with more users, longer flying time, and more iteration rounds [2]. Similarly, deep reinforcement learning (DRL) frameworks [6], [7], [8], [9], [10] may be limited in their ability to explore all possible paths over a large area within a limited number of simulation rounds. Therefore, their results may not represent optimal trajectories.

A. Related Work

In order to satisfy the minimum signal-to-noise ratio (SNR) requirements, UAVs must fly a certain distance to approach ground equipment for transmission links. The flight trajectory employed can significantly affect the UAV's data collection. However, designing UAV trajectories is typically more challenging due to the involvement of continuous space, which leads to a myriad of design variables relating to both trajectory and communication [2], [3]. To address this issue, a suggested approach is to estimate the path of the UAV by using a continuous linear trajectory consisting of a sequence of connected line segments with a finite number of 3D waypoints [2]. There are two trajectory discretization techniques [2]. *1) Time Discretization (TD)* [5], [6], [7], [8], [9], [10], [11], [12], [13], [14]: The time horizon for flight is divided into equal time slots. This ensures that the position of the UAV remains relatively constant during each time slot in comparison to the distances between all devices and the UAV [4]. In each time slot, one or more devices can upload data simultaneously to the UAV. *2) Path Discretization (PD)* [15], [16], [17], [18], [19]: The UAV trajectory is divided into successive line segments of generally unequal length, connected by hovering positions (waypoints). The duration of time allocated by the UAV for each line segment may vary [3]. The UAV gathers data produced by the ground equipment at each hovering location. In addition, optimizing an increasing number of waypoints generally leads to a higher level of complexity in designing UAV trajectories [3]. Therefore, a UAV trajectory design that uses PD will typically result in a lower computational complexity than one that uses TD.

Based on the two trajectory discretization techniques mentioned above, recent research on the co-design of trajectory and communication in UAV data collection can be categorized into three optimization goals: 1) maximizing energy efficiency [6], [12], [13], [16], [17], [18]; 2) maximizing throughput/data rate [3], [7], [9], [10], [11], [14], [20]; and 3) minimizing latency [4], [8], [19], [21]. In [6], researchers presented a joint design for allocating frequency bands and determining the 3D trajectory of the UAV for mobile ground users (GUs) in a UAV-based communication system. The aim was to promote fairness and energy efficiency. In [14], the objective was to tackle the issue of deploying UAVs in 3D space while simultaneously optimizing the overall user rate and fulfilling on-board energy and flight duration limitations. Furthermore, timely data collection is equally critical as system throughput. In [4], Samir et al. optimized the flight path of a single UAV and allocated radio resources for maximizing the number of connected IoT devices, each with its own deadline for uploading data. In [19] and [21], a measure of information freshness called Age of Information (AoI) was introduced. For example, in [19], the mission completion time of the UAV was minimized by a combination of UAV flight speed, hover position, and visit sequence optimization, while considering the AoI of the data in the survey area.

The above optimization models include user time schedule and assignment, UAV trajectory planning, transmission power control, etc., which are strongly interrelated and generally difficult to solve. For example, in [16], the trajectory planning of the UAV, which includes the sensor serving orders and the UAV's hovering positions, was optimized in conjunction with the upload power allocation of the sensors. To address these issues, the standard traveling salesman problem (TSP) was utilized to formulate and solve the optimal serving orders of the sensors. In addition, the SCA method was used to obtain the hovering positions of the UAV and the pattern search method was used to optimize the transmission power. Specifically for the trajectory problem, the SCA [2], [3], [4], [11], [13], [16], [21] and block coordinate descent (BCD) [2] techniques have been proposed, e.g., the SCA method iteratively finds the optimal trajectory by constructing the surrogate functions of the original function. For PD-based trajectory optimization, the TSP [21] and the pickup-and-deliver problem (PDP) [2] have been introduced to initialize UAV path planning and determine the amount of time to allocate at each UAV location along the path. On the other hand, DRL algorithms can reach an optimization solution by maximizing the expected cumulative reward without transforming a non-convex problem into a convex one [22], [23]. Recently, a number of DRL-based frameworks for UAV communication have been proposed to reduce packet loss [8], improve overall throughput [7], [10], [24], and increase energy efficiency [12], [17]. In [9], a scheme based on deep Q-network (DQN) was presented to maximize the total data rate of the users. This was achieved by determining the UAV's next waypoint and the transmission power of ground equipment in a discrete space. In [8], researchers developed a flight control scheme based

on deep deterministic policy gradient (DDPG) to minimize data packet loss by predicting the UAV's next position and velocity, and the devices selected for data collection in a continuous space. Moreover, in [6], [9], [22], [25], and [26], DRL algorithms were employed to concurrently optimize multiple objectives in the UAV-assisted network. To illustrate, in [26], the primary objective was to diminish the average latency and enhance the service success rate through the integration of UAV server-user associations, bandwidth, and computational resource allocation policies.

B. Contributions

This paper analyzes a data collection problem in UAV communications. Our optimization objective is to maximize data throughput while ensuring low latency performance. To account for the limited on-board energy of the UAV, we limit the mission duration of the UAV. A new equation has been developed to calculate the throughput of data gathering networks by allocating resource blocks to ground devices. The method divides joint optimization into two separate stages: planning the trajectory and allocating communication resources. To decrease the computational complexity of trajectory optimization, we optimize each flight path segment separately. This involves separating the nonconvex optimization into convex subproblems. This paper's main contributions are summarized below.

- The data collected from UAV-assisted communication is presented as two components: the average rate per unit of bandwidth for all devices, and the size of the allocable resource block characterized by bandwidth and duration during the entire flight duration. For the first time, we demonstrate that maximizing the average amount of data collected during a flight duration is equivalent to minimizing the flight distance of a UAV, provided that each device is within the UAV's maximum allowable horizontal coverage when it communicates with the UAV.
- An advanced hierarchical clustering algorithm is proposed for grouping randomly placed IoT devices into multiple disjoint clusters, utilizing the maximum horizontal coverage of the UAV instead of load balancing among clusters. Furthermore, the proposed clustering algorithm eliminates the requirement of predefining a certain number of clusters and guarantees that the UAV services each device while enabling the minimum flight distance.
- A segmented path optimization scheme based on TSP is proposed to decompose non-convex trajectory scheduling into a sequence of convex optimizations for path segments. In each round, TSP is used to achieve the initial path planning. Following that, the optimization process begins at the first hovering point by minimizing the two adjacent path segments connected by that point, while maintaining all other hovering positions. This process continues until all hovering positions are updated sequentially. The UAV's flight distances decrease with each round, eventually leading to the attainment of an optimal trajectory after a few iterations.
- Given the optimal trajectory, the communication optimization is transformed into the joint optimization of hovering time for each cluster and bandwidth for each device in the clusters using Frequency Division Multiple Access (FDMA), and upload time optimization for each device by means of Time Division Multiple Access (TDMA), respectively. The issue of load balancing between clusters can be resolved by optimizing the UAV hovering time for each cluster to upload data, without controlling cluster size.
- We provide two different device distribution scenarios to demonstrate different trajectory representations resulting from multiple co-designs of trajectory and communication in a UAV-based data collection network. Through our comparison of SCA-based schemes and DRL-based frameworks, we demonstrate that the suggested joint UAV trajectory and communication optimization achieves a significantly lower upload failure rate and favorable data collection performance with reduced complexity.

C. Paper Organization

The structure of the paper is as follows: Section II is an introduction to the system model and the problem formulation. A resource block based optimization model is presented in Section III. Sections IV and V outline the UAV trajectory and communication optimization schemes, respectively. Section VI analyzes the numerical results. Finally, in Section VII, the study concludes and potential areas for future research are discussed.

II. System Model and Problem Statement

A. System Model

Suppose a scenario where a UAV is deployed to gather information from K sensor nodes (SNs) on the ground. Due to the limited on-board energy of the UAV, we assume that the UAV completes a data collection mission within a given time T and flies at a fixed altitude H and a constant speed V. The coordinate of the kth SN, referred to as $q_k = [x_k, y_k, 0] \in \mathbb{R}^3$, $k \in [1, K]$, is invariant within T. The UAV initiates its flight from a designated start point u_{str} and traverses the area according to a predetermined path $\mathbf{U} = \{u(t)|t \in [0, T]\}$ until reaching the designated end point u_{end}. Here, $u(t) = [x(t), y(t), H] \in \mathbb{R}^3$ denotes the UAV's position at time t. Furthermore, the sensed data of SN k is packed into an information packet of a specific size, Q_k^{th}, and must be uploaded to the UAV before the end of this flight duration, otherwise this SN is considered to have failed to upload data. Here, the time of compressing and packaging data is ignored. B denotes the bandwidth of the system. The UAV's data from SN k during the UAV flight duration T is represented by

$$Q_k = \int_0^T B_k(t)\log_2\left(1 + \frac{P_k(t)\beta_0}{\|u(t) - q_k\|^2\sigma^2}\right)dt, \quad (1)$$

where $P_k(t)$ and $B_k(t)$ are the transmit power and the allocated bandwidth of SN k at time t, respectively, $\|\cdot\|$ is the Euclidean norm, and σ^2 is the additive white Gaussian noise (AWGN) power. We consider UAV-to-SN communication channels as LoS linkages that are extendable to non-line-of-sight (NLoS) channel models [4], [6], [7], [9], [10], [14], [15], [17], [19]. β_0 is path loss at 1m reference distance.

According to (1), the total data collected by the UAV from K SNs during T is

$$Q = \sum_{k=1}^{K} \int_0^T B_k(t) \log_2 \left(1 + \frac{P_k(t)\beta_0}{\|u(t) - q_k\|^2 \sigma^2}\right) dt. \quad (2)$$

B. Problem Formulation

We study the bandwidth, upload time, and power allocation as well as the trajectory for maximizing the average data collection of SNs during a UAV flight duration. Let $\mathbf{B} = \{B_k(t) | t \in [0, T], k \in [1, K]\}$ and $\mathbf{P} = \{P_k(t) | t \in [0, T], k \in [1, K]\}$, and then the formulation of the optimization problem will be

$$P1: \max_{\mathbf{U},\mathbf{P},\mathbf{B}} \frac{1}{K} \sum_{k=1}^{K} \int_0^T B_k(t) \log_2 \left(1 + \frac{P_k(t)\beta_0}{\|u(t) - q_k\|^2 \sigma^2}\right) dt \quad (3)$$

$$\text{s.t.} \quad Q_k \geq Q_k^{th}, \forall k, \quad (3a)$$

$$0 \leq P_k(t) \leq P^{\max}, \forall k, t, \quad (3b)$$

$$\frac{P_k(t)\beta_0}{\|u(t) - q_k\|^2 \sigma^2} \geq \gamma^{th}, \forall k, t, \quad (3c)$$

$$B_k(t) \geq 0, \forall k, t, \quad (3d)$$

$$u(0) = u_{str}, u(T) = u_{end}, \quad (3e)$$

where $P^{\max}$ denotes the maximum upload power of SN and γ^{th} denotes the required minimum instantaneous signal-interference-ratio (SINR). (3a) shows that during T, each SN must upload all its generated data to the UAV. (3b) indicates that the transmit power of each SN must be not greater than its maximum transmit power. (3c) indicates that the instantaneous received SINR of the UAV from each SN must meet the minimum requirement. (3d) indicates a bandwidth of 0 or greater allocated for each SN. (3e) specifies that the UAV departs from the starting point and returns to the ending point.

In general, solving $P1$ is inexorable because of trajectory variables that are infinite in time, i.e., $u(t)$. We adopt the PD-based trajectory scheme. Let $\hat{\mathbf{U}} = \{u_i\}$ denote the set of hovering positions, where $u_i = [x_i, y_i, H]$ is UAV's coordinate at hovering point i and $N = \left|\hat{\mathbf{U}}\right|$ denotes the number of hovering points. As illustrated in Fig. 1, the trajectory of the UAV is indicated by $\Pi = [u_0, u_1, \ldots, u_n, \ldots, u_N, u_{N+1}]$, which represents all possible sequences of visiting hovering points during the UAV flight duration and is a permutation of $\hat{\mathbf{U}}$ in addition to $u_0 = u_{str}$ and $u_{N+1} = u_{end}$. Along the trajectory Π, segment n connects hovering points u_{n-1} and u_n, and $T_n = T_n^f + T_n^h$ denotes the UAV travelling time through segment n, which includes the flight time T_n^f from hovering point positions u_{n-1} to u_n and the hovering time T_n^h at hovering position u_n. Therefore, the total UAV flight duration T is given by $T = T^h + T^f = \sum_{n=1}^{N} T_n + T_{N+1}$ where T_{N+1} is the flight time from u_N to u_{end}, and $T^h = \sum_{n=1}^{N} T_n^h$ and $T^f = \sum_{n=1}^{N+1} T_n^f$ respectively denote the total hovering time and the total flight time during a flight duration T.

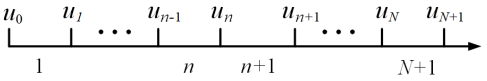

Fig. 1. 1D Illustration of Discretized trajectory.

Assume that channel state information (CSI) can be accurately obtained by the UAV. Additionally, each SN is associated with the UAV uniquely at one hovering point during T, and the channel gain between each SN and the UAV remains constant during their association time. Whether using TDMA, FDMA or any other communication mode, a mobile device must be assigned a specific resource block of time and bandwidth to enable its data transmission. Here, we assume that SN k at hovering point i is allocated an upload time $\delta_{i,k}$ and a bandwidth $B_{i,k}$. Let $J_i = \{\delta_{i,k} > 0 | k \in [1, K]\}$ be the cluster (set) of the SNs within the coverage of hovering point i, specifically $\delta_{i,k} = 0$ indicating that SN k keeps silent at hovering point i. Thus, the amount of collected data from SN k at hovering point i can be expressed by

$$\hat{Q}_{i,k} = \underbrace{B_{i,k}\delta_{i,k}}_{\substack{\text{Resource block} \\ \text{for a SN}}} \underbrace{\log_2 \left(1 + \frac{P_{i,k}\beta_0}{\|u_i - q_k\|^2 \sigma^2}\right)}_{\text{Upload rate per unit of bandwidth for a SN}}, \quad (4)$$

where $P_{i,k}$ denotes the transmit power of SN k at hovering point i. According to (4), the data collection from cluster J_i is represented as

$$\hat{Q}_i = \sum_{k \in J_i} \delta_{i,k} B_{i,k} \log_2 \left(1 + \frac{P_{i,k}\beta_0}{\|u_i - q_k\|^2 \sigma^2}\right). \quad (5)$$

Let $\hat{\mathbf{P}} = \{P_{i,k} | i \in [1, N], k \in [1, K]\}$, $\hat{\mathbf{B}} = \{B_{i,k} | i \in [1, N], k \in [1, K]\}$, $\Upsilon = \{\delta_{i,k} | i \in [1, N], k \in [1, K]\}$ and $\mathbf{J} = \{J_i | i \in [1, N]\}$. According to (5), problem $P1$ can be converted into a joint optimization consisting of bandwidth $\hat{\mathbf{B}}$, upload time Υ and power allocation $\hat{\mathbf{P}}$ in addition to SN clustering $\mathbf{J}$, hovering positions $\hat{\mathbf{U}}$ and trajectory scheduling Π. We rewrite $P1$ by

$$P2: \max_{\hat{\mathbf{U}},\mathbf{J},\Pi,\hat{\mathbf{B}},\Upsilon,\hat{\mathbf{P}}} \hat{Q}_{avg} = \frac{1}{K} \sum_{i \in \mathbf{J}} \sum_{k \in J_i} \delta_{i,k} B_{i,k} \log_2 \left(1 + \frac{P_{i,k}\beta_0}{\|u_i - q_k\|^2 \sigma^2}\right) \quad (6)$$

$$\text{s.t.} \quad \hat{Q}_{i,k} \geq Q_k^{th}, \forall k, i, \quad (6a)$$

$$\delta_{i,k} \geq 0, \forall k, i, \quad (6b)$$

$$0 \leq P_{i,k} \leq P^{\max}, \forall i, k, \quad (6c)$$

$$\frac{P_{i,k}\beta_0}{\|u_i - q_k\|^2 \sigma^2} \geq \gamma^{th}, \forall i, k, \quad (6d)$$

$$B_{i,k} \geq 0, \forall k, i, \quad (6e)$$

$$u_0 = u_{str}, u_{N+1} = u_{end}, \quad (6f)$$

$$\sum_{i \in \mathbf{J}} T_i^h \leq T^h, \quad (6g)$$

$$\sum_{k \in J_i} B_{i,k}\delta_{i,k} \leq B T_i^h, \forall i. \quad (6h)$$

Here, for easy analysis, we use $\delta_{i,k}$ to represent the SN scheduling variable, i.e., when $\delta_{i,k} > 0$, user k is connected with the UAV in hovering point i; otherwise, $\delta_{i,k} = 0$. (6g) states that the sum of the total time in the hovering state in

all clusters shall not exceed the total UAV hovering time. (6h) stipulates that the aggregate of the resource blocks assigned to all SNs within a cluster must not exceed the total number of resource blocks allocated to the cluster.

From (6), given other decision variables, the amount of data collection by the UAV increases with increasing transmit power, so the maximum transmit power $P^{\max}$ provides the best power allocation solution. However, the communication design for $\hat{\mathbf{B}}$ and Υ and the UAV trajectory plan of Π, $\hat{\mathbf{U}}$ and $\mathbf{J}$ are coupled, which cannot be solved directly by existing convex optimization solvers.

III. Resource Block-Based Joint Optimization Model

According to problem $P2$, each SN's transmit power is set to maximum. We consider the SNs in a cluster as a single entity of uploading data. The length of time the UAV hovers at hovering point i is assumed to be T_i^h, so a wireless resource block with the size of BT_i^h is allocated to cluster J_i for uploading data. Thus, equation (5) can be rewritten as

$$\hat{Q}_i \triangleq \underbrace{BT_i^h}_{\substack{\text{Resource block}\\ \text{for a cluster}}} \underbrace{\frac{1}{|J_i|}\sum_{k\in J_i}\log_2\left(1+\frac{P^{\max}\beta_0}{\|u_i-q_k\|^2\sigma^2}\right)}_{\substack{\text{Average upload rate per unit of}\\ \text{bandwidth for SNs in a cluster}}}, \quad (7)$$

where $|J_i|$ is the number of SNs in J_i.

Similarly, data collection from all SNs can be obtained during a flight duration, expressed as

$$\hat{Q} \triangleq \underbrace{BT^h}_{\substack{\text{Resource block}\\ \text{during a}\\ \text{flight duration}}} \underbrace{\frac{1}{K}\sum_{i\in\mathbf{J}}\sum_{k\in J_i}\log_2\left(1+\frac{P^{\max}\beta_0}{\|u_i-q_k\|^2\sigma^2}\right)}_{\substack{\text{Average upload rate per}\\ \text{unit of bandwidth for all SNs}}}. \quad (8)$$

From equation (8), it can be inferred that increasing the resource block size or the average upload rate of all SNs can enhance the amount of data obtained by the UAV. However, with fixed values of T and B, lengthening the hovering duration T^h is bound to reduce the UAV flight distance, which, in turn, will lead to a decrease in the average data upload rate of the SNs, and vice versa. To overcome this issue, we propose a lemma below by deriving an approximation function from equation (8).

Lemma 1: In UAV-assisted data collection networks that employ the PD-based trajectory scheme, increasing the UAV's hover time (or decreasing its flight time) will increase the amount of data collected during a given flight duration, if the horizontal distance between the UAV and its associated SN remains $(\frac{r_{i,k}}{H})^2 \ll 1, \forall k \in J_i, \forall i \in \mathbf{J}$ at each hovering position.

Proof: See Appendix.

Lemma 1 states that the problem $P2$ can be divided into two steps: Firstly, the flight distance of the UAV is minimized, while ensuring that each SN remains within the maximum horizontal coverage of the UAV, denoted by

$$P3: \min_{\hat{\mathbf{U}},\Pi,\mathbf{J}} dist(\hat{\mathbf{U}}) \quad (9)$$

$$\text{s.t.} \quad r_{i,k} \le r_{\max}, \quad \forall k \in J_i, \forall i \in \mathbf{J}, \quad (9a)$$

6(f),

where $dist(\hat{\mathbf{U}})$ denotes the flight distance along all hovering positions $\hat{\mathbf{U}}$ and $r_{\max}$ satisfies $r_{\max} \leqslant \left(\frac{P^{\max}\beta_0}{\gamma^{th}\sigma^2} - H^2\right)^{\frac{1}{2}}$ and $(\frac{r_{max}}{H})^2 \ll 1$.

With the optimized UAV trajectory of Π^*, $\hat{\mathbf{U}}^*$ and $\mathbf{J}^*$ by solving $P2$, we can obtain the optimal duration for the UAV to hover, $(T^h)^*$, throughout the entire flight duration. Subsequently, the next step involves maximizing the average data collection by optimizing the bandwidth $\hat{\mathbf{B}}$ and upload time Υ. This can be expressed as

$$P4: \max_{\Upsilon,\hat{\mathbf{B}}} \frac{1}{K}\sum_{i\in\mathbf{J}^*}\sum_{k\in J_i^*}\delta_{i,k}B_{i,k}\log_2\left(1+\frac{P^{\max}\beta_0}{\|u_i^*-q_k\|^2\sigma^2}\right) \quad (10)$$

$$\text{s.t.} \quad \sum_{i\in\mathbf{J}^*}\sum_{k\in J_i^*}\delta_{i,k} = (T^h)^*, \quad (10a)$$

$$\sum_{k\in J_i^*} B_{i,k} = B \quad \forall i,$$

6(a), 6(b), 6(e)., (10b)

IV. Optimization of UAV Flight Trajectory

Optimization problem $P3$ involving trajectory and user scheduling is a NP-hard problem. Generally, the more waypoints the UAV must hover, the longer the UAV's flight distance. Therefore, reasonable clustering algorithm to shorten the flight distance while covering all SNs is crucial in UAV trajectory design.

We propose a cluster coverage plus segmented path optimization (CSegP) scheme to solve problem $P3$, which is decomposed into two modules: 1) a clustering module with the objective of classifying the SNs to obtain the cluster sets $\mathbf{J}$ and the number of clusters (hovering points) N; and 2) a trajectory scheduling module with the objective of determining the hovering positions $\hat{\mathbf{U}}$ for each cluster and the flight trajectory Π along all hovering positions $\hat{\mathbf{U}}$.

A. Clustering Module

Based on $P3$, the sole determinant of the clustering algorithm is the maximum radius of horizontal coverage of the clusters. In light of the fact that the hierarchical clustering approach [27], [28] merges the most comparable clusters by computing the Euclidean distance between them, we revise the method by updating the criteria for determining the merging strategy and terminating the clustering process. Advanced hierarchical clustering presents several advantages over other clustering algorithms like k-means [29] and affinity propagation (AP) [30]. These advantages include its ability to 1) handle clusters of various sizes and densities, and 2) not requiring the number of clusters to be specified.

Given two clusters J_i and J_j, their distance is defined as

$$d(J_i, J_j) = \max_{x\in J_i, z\in J_j}\|u_x - u_z\|. \quad (11)$$

The stop criterion is defined as

$$\min_{\forall J_i, J_j} d(J_i, J_j) > 2r_{\max}. \quad (12)$$

For the detailed procedure of the advanced hierarchical clustering algorithm, see Algorithm 1.

Algorithm 1 Implementation Process of the Advanced Hierarchical Clustering

Input:

Cluster distance function according to (11)
A criterion to stop clustering $\kappa = 2r_{\max}$
Each SN as a separate cluster $\mathbf{J}=\{J_i | i \in [1, K]\}$
for $i = 1, 2, \ldots, K$ **do**
  for $j = i+1, \ldots, K$ **do**
    $D(i, j) = d(J_i, J_j)$
    $D(j, i) = D(i, j)$
  end for
end for
Setting the number of clusters: $N = K$
while $N > 1$ **do**
  Finding the two nearest clusters J_i^* and J_j^*, with a distance of $d_{\min}$
  if $d_{\min} > \kappa$ **then**
    End the clustering process
  end if
  Merge J_i^* and J_j^*: $J_i^* = J_i^* \cup J_j^*$
  for $j = j^*+1, j^*+2, \ldots, N$ **do**
    Renumber cluster J_j to J_{j-1}
  end for
  Clear row j^* and column j^* from D.
  for $j = 1, 2, \ldots, N-1$ **do**
    $D(i^*, j) = d(J_{i^*}, J_j)$
    $D(j, i^*) = D(i^*, j)$
  end for
  $N = N - 1$
end while

Output: Cluster set: $\mathbf{J}$

B. Trajectory Scheduling Module

Through the clustering module, we obtain the SN cluster set $\mathbf{J}^*$ and the number of clusters N. Then, the trajectory scheduling for problem $P3$ is first solved by finding the optimal hovering positions $\hat{\mathbf{U}}$ for all clusters. Once $\hat{\mathbf{U}}$ is determined, optimizing the trajectory Π along the hovering positions $\hat{\mathbf{U}}$ is similar to the TSP to find the shortest path [31]. However, the two optimizations are combined and therefore difficult to handle independently.

We propose a segmented path optimization scheme based on the TSP by following two steps: 1) finding the shortest flight distance along the hovering points by solving the TSP; and 2) sequentially optimizing one hovering position while keeping other positions fixed by minimizing the two adjacent path segments connected by that point. The trajectory generated by each step of the operation, in which either all hovering points are permuted or the position of one hovering point is optimized, becomes shorter than those in the preceding steps. This results in the iterative convergence of the optimal trajectory. Specific steps include **Step 1:** Initializing all hovering positions of the UAV.

All hovering positions in the 0th round are initialized to be $\hat{\mathbf{U}}^0 = \{u_i = \frac{1}{|J_i^*|} \sum_{k \in J_i^*} q_k | i \in [1, N]\}$.

Step 2: Permutation of all hovering points via solving the TSP.

We solve the TSP to find the rth round trajectory with the shortest distance, $\Pi^r = \left[u_0, u_1^r, \cdots, u_N^r, u_{N+1}\right]$, along the hovering positions $\hat{\mathbf{U}}^r$.

Step 3: Sequential optimization of hovering positions along the trajectory.

Along the rth round trajectory, Π^r, shown in Fig. 1, starting from the initial position, we can achieve the nth best hovering location, $(u_n^r)^*$, by minimizing the length of segments n and $n+1$. This can be accomplished by taking into account the optimized previous position, $(u_{n-1}^r)^*$, in this round and its subsequent position, u_{n+1}^r. Optimizing for this scenario can be expressed as

$$P5: \min_{u_n} \|u_n - (u_{n-1}^r)^*\|^2 + \|u_{n+1}^r - u_n\|^2 \tag{13}$$

$$\text{s.t.} \quad \|u_n - q_k\|^2 \le r_{\max}^2 + H^2, k \in J_n^*. \tag{13a}$$

Since (13) is a convex function, the method of Lagrange multipliers [32] is introduced as

$$L(u_n, \lambda_k) = \|u_n - (u_{n-1}^r)^*\|^2 + \|u_{n+1}^r - u_n\|^2 + \sum_{k \in J_n^*} \lambda_k (\|u_n - q_k\|^2 - r_{\max}^2 - H^2).$$

The necessary conditions for optimization are written as

$$\begin{cases} \dfrac{\partial L(u_n, \lambda_k)}{\partial u_n} = \\ 4u_n - 2(u_{n-1}^r)^* - 2u_{n+1}^r + 2\sum\limits_{k \in J_n^*} \lambda_k (u_n - q_k) = 0, \\ \dfrac{\partial L(u_n, \lambda_k)}{\partial \lambda_k} = \|u_n - q_k\|^2 - r_{\max}^2 - H^2 = 0, \\ \lambda_k \ge 0. \end{cases}$$

We can obtain

$$\begin{cases} (u_n^r)^* = \dfrac{(u_{n-1}^r)^* + u_{n+1}^r + \sum\limits_{k \in J_n^*} \lambda_k{}^* q_k}{2 + \sum\limits_{k \in J_n^*} \lambda_k{}^*}, \\ \lambda_k{}^* \ge 0. \end{cases} \tag{14}$$

By solving $P5$, the hovering positions along the trajectory Π^r are iteratively updated to the final position u_N, and we can obtain the next round set of hovering positions, $\hat{\mathbf{U}}^{r+1} = \{(u_i^r)^* | i \in [1, N]\}$.

Repeating **Step 2** and **Step 3**, we get $dist(\Pi^0) \ge dist(\Pi^1) \ge \cdots \ge dist(\Pi^r) \ge dist(\Pi^{r+1}) \ge \cdots$ until the optimal flight trajectory is reached after a number of rounds.

V. Communication Optimization

The UAV's optimal hover time, $(T^h)^*$, and the upload rate of each SN, $R_k^*, k \in [1, K]$, via the optimal UAV trajectory have been determined. In the TDMA manner, the UAV receives data one at a time from the SNs in a cluster. According to equation (5), the total data collected by the UAV during a flight duration can be rewritten as

$$\hat{Q}^{TDMA} = B \sum_{i \in \mathbf{J}} \sum_{k \in J_i} \delta_{i,k} \log_2 \left(1 + \frac{P^{\max} \beta_0}{\|u_i - q_k\|^2 \sigma^2}\right). \tag{15}$$

Similarly, in the FDMA manner, the UAV receives data from SNs within a cluster on different bandwidths at the same time.

According to equation (5), the total data collected by the UAV during its entire flight time can be described as

$$\hat{Q}^{FDMA} = \sum_{i\in\mathbf{J}} T_i^h \sum_{k\in J_i} B_{i,k}\log_2\left(1+\frac{P^{\max}\beta_0}{\|u_i-q_k\|^2\sigma^2}\right), \quad (16)$$

where $B = \sum_{k\in J_i} B_{i,k}, \forall i$.

According to (15) and (16), problem $P4$ is transformed into optimizing the upload time per SN in the TDMA manner and the bandwidth per SN in a cluster and the hovering time per cluster in the FDMA manner, respectively. For simplicity, we focus on the TDMA method (the optimal outcomes are achieved similarly in the FDMA manner). Once the optimized set of clusters $\mathbf{J}^*$ is determined, we can designate δ_k as the upload time duration of SN k during T. Let $\hat{\Upsilon} = \{\delta_k | k \in [1, K]\}$. From equation (15), $P4$ can be expressed as

$$P6: \max_{\hat{\Upsilon}} \hat{Q}_{avg} = \frac{B}{K}\sum_{k=1}^{K}\delta_k R_k^* \quad (17)$$

$$\text{s.t.} \quad \delta_k B R_k^* \geq Q_k^{th}, \quad \forall k \in [1, K], \quad (17a)$$

$$\delta_k \geq 0, \quad \forall k \in [1, K], \quad (17b)$$

$$\sum_{k=1}^{K}\delta_k = (T^h)^*, \quad (17c)$$

where $R_k^* = \log_2\left(1+\frac{P^{\max}\beta_0}{\|u_i^*-q_k\|^2\sigma^2}\right), k \in [1, K]$.

Problem $P6$ is a first-order polynomial with respect to $\hat{\Upsilon}$. Sorting the upload rates of all SNs in a descending order, we obtain $R_1^*, \ldots, R_k^*, \ldots, R_K^*$. To collect the maximum amount of data possible, we set $\delta_1^* = (T^h)^* - \sum_{k=2}^{K}\delta_k^*$ and $\delta_k^* = \frac{Q_k^{th}}{BR_k^*}, k > 1$. This requires satisfying $\sum_{k=1}^{K}\frac{Q_k^{th}}{BR_k^*} \leq (T^h)^*$, otherwise, we minimize the number of SNs with failed data uploads and set $\delta_1^* = \frac{Q_1^{th}}{BR_1^*}, \cdots, \delta_{\hat{k}}^* = (T^h)^* - \sum_{j<\hat{k}}\delta_j^*, \delta_{\hat{k}+1}^* = 0, \cdots, \delta_K^* = 0$.

VI. Numerical Results

Numerical results confirming the effectiveness of our proposed algorithm are presented in this section. Our study explores a network assisted by a UAV, wherein all SNs are scattered in a random manner in a $200 \times 200\text{m}^2$ square area [12]. The UAV starts flying from the given coordinates $u_{str} = [0, 0, 100]^T$ and finishes its flight at $u_{end} = u_{str}$. We set the average packet length of K SNs to $Q_{avg}^{th} = \frac{1}{K}\sum_{k=1}^{K} Q_k^{th}$. The normal setting of the parameter values is shown in TABLE I. There may be changes to some of the parameter settings. The specific changes are explained in each figure. In each simulation, we generated 100 flight durations with varying SN distributions for the purpose of validation. The computer used for simulations had an Intel i7, 2.9 GHz processor and 16 GB RAM. The DRL algorithms were executed in PyCharm 2022.3.2, while the other algorithms were executed in MATLAB 2022b.

TABLE I
Simulation Parameters

Parameters	**Values in general**
Flight duration T	100s [3], [4]
Maximum transmit power of SN $P^{\max}$	0.2W [3]
Velocity of UAV V	20m/s [3], [12]
Receiver noise power σ^2	10^{-13}W/Hz [12]
Bandwidth B	5kHz
Maximum horizontal coverage radius of UAV $r_{\max}$	15m
Power gain of the channel at the reference distance of 1 m β_0	-60dB [3], [19]
Flight altitude of UAV H	100m [3], [10]
Number of SNs K	10
Average packet length of SNs Q_{avg}^{th}	0.5kbit
Minimum SINR of SN γ^{th}	22dB
Fully-charged battery energy of UAV E_{max}	10^5J [6]

A. Comparison of Different UAV Trajectory and Communication Co-Designs

To support the conclusion of Lemma 1 and evaluate the effectiveness of our proposed CSegP scheme, we use the SCA method [4] to obtain the minimum path as the optimal solution for problem P3, which we term MinPath-SCA. We introduce two benchmarks [3]: PD-MaxRate and TD-MaxRate, both aimed at maximizing the minimum achievable rate among all SNs and solved using the SCA method. Below is a brief description of them.

- PD-MaxRate uses the PD-based trajectory, with the given number of hovering positions, N.
- TD-MaxRate utilizes the TD-based trajectory, dividing the given flight duration of $[0, T]$ into M equally sized time slots with enough short lengths of δ_t. Setting the maximum segment length, $\Delta_{\max} = 2{*}r_{\max} = 30$m [2], [3], we can obtain $\delta_t = \lceil\Delta_{\max}/V\rceil = 1.5$s and $M = \lceil T/\delta_t\rceil = 67$ where $\lceil\cdot\rceil$ is the ceiling function.

In addition, two DRL-based frameworks are also used as benchmarks. In both cases, the remaining energy of the UAV is calculated in accordance with equation (27) in [6]. Fig. 2 illustrates the training curves for the cumulative reward of DQN and DDPG.

- DQN [7]: The state space is defined by the current location and remaining battery budget of the UAV and the locations of the SNs. The action space is defined by the 7 flight directions of the UAV (left, right, forward, backward, up, down, hovering). The reward function comprises two components: the instantaneous data collected from all nodes at a given time step and a penalty imposed by the safety controller to ensure that the UAV reaches the terminal point. Please refer to equation (7) in [7].
- DDPG [6]: The state space includes the locations of the SNs, the UAV's current location and energy and the destination location. The action is UAV velocity (including the UAV speed and flight direction). The shaped reward refers to equation (49) in [6].

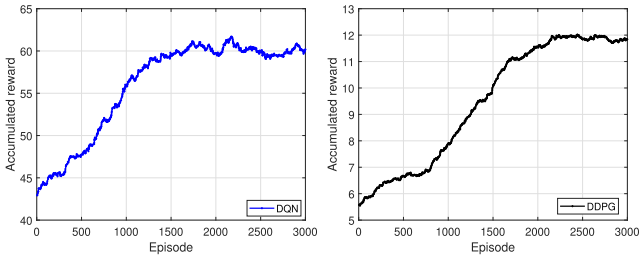

Fig. 2. Accumulated reward versus training episode using DQN and DDPG.

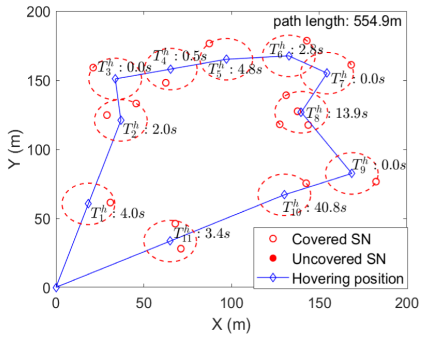

Fig. 3. Optimized UAV trajectory for 16 SNs using proposed CSegP.

1) The Optimized UAV Trajectories by Different Schemes: Fig. 3 depicts the clustering and trajectory planning of the proposed CSegP scheme for 16 SN scenarios, illustrating the hovering time for each cluster. As illustrated in Fig. 3, the designated hovering time for the 3rd, 7th, and 9th clusters is 0 seconds. The results demonstrated that six of the 16 SNs were unable to complete the data upload within the specified time of T. Furthermore, Figs. 4(a)-(g) and Figs. 4(h)-(j) illustrate the optimized UAV trajectories by different schemes, demonstrating the two distribution scenarios for 10 SNs, respectively. First, based on Figs. 4(a)-(b), it is apparent that the UAV flies to close to each SN in turn, so that TD-MaxRate and PD-MaxRate achieve a higher average SN rate compared to other schemes. The TD-MaxRate scheme achieves the highest average rate of the SNs by allowing the UAV to control its trajectory near the SNs more flexibly through characterizing the trajectory with more designable slots. Second, from a visual analysis of Figs. 4(c)-(d), it is evident that owing to the implementation of a limited number of exploration rounds, the use of DQN and DDPG does not successfully guide the UAV convergence to each node, despite having sufficient designable slots. Furthermore, the smoothness of the trajectory in the DDPG method outperforms that in the DQN method. This result is attributed to the continuous nature of the output actions in the DDPG approach, which enhances the stability of the trajectory output. Third, it is apparent from Figs. 4(e)-(f) that the MinPath-SCA scheme with equivalent designable hovering positions (i.e. $N = 8$) generates two distinct UAV trajectories for Case 1, wherein one SN is not served in Fig. 4(e). This issue arises from the varying initial settings of the hovering positions implemented by the SCA method. Furthermore, we can observe in Fig. 4(g) that the proposed CSegP scheme optimizes N to 8 for Case 1 and its UAV path matches that of the MinPath-SCA scheme shown in Fig. 4(f). Finally, to show the effect of the number of designable hovering positions on the UAV trajectory, the MinPath-SCA scheme in Case 2 is set to N=8, 9 and 10. It can be observed from Fig. 4(h) that there are two SNs that are not served when N=8, while as shown in Figs. 4(i)-(j), the MinPath-SCA scheme with N=10 yields a longer path than with N=9. Additionally, the CSegP scheme optimizes N to 9 and achieves the identical path as the MinPath-SCA scheme with N set to 9. The above figures indicate that CSegP can achieve optimal trajectories without experiencing optimization failures caused by an incorrect number of hover points or UAV position initialization, as seen in the SCA method.

2) System Performance When Changing the Number of SNs: The number of designable hovering positions for both PD-MaxRate and MinPath-SCA is fixed at $N = 10$. In Figs. 5(a)-(c), we analyze the variation curves of average data collection, SN failure rate, and runtime as the number of SNs varies. Due to the negligible runtime of the DRL-based method, the runtime lines of DDPG and DQN are not plotted in Fig. 5(c). The most important observations can be summarized as follows. First, from Figs. 5(a)-(b), it is evident that for the PD-based trajectory schemes including PD-MaxRate, MinPath-SCA and CSegP, the average data collections decrease as K increases. Additionally, the SN failure rates remain constant at 0 from $K = 6$ to 10, followed by an increase from $K = 10$. Eventually, the failure rates of both MinPath-SCA and CSegP became very close. This was due to the fact that the PD-based UAV trajectories with more SNs require the UAV to fly longer distances, resulting in less time for data uploading. However, for the TD-based trajectories like TD-MaxRate, DQN, and DDPG, the average data collection and SN failure rate show minimal change as K increases. This is because when K is small, there are many free slots in the TD-based trajectories, and as K increases, the newly added SNs will upload their data in these free slots, so that if Q_{avg}^{th} is fixed, the SN failure rate and the average data collection do not change. Second, as shown in Fig. 5(c), the runtimes for TD-MaxRate and CSegP consistently increase as the value of K increases. In comparison, PD-MaxRate and MinPath-SCA demonstrate longer runtimes at $K = 6$ and $K = 8$ than at $K \geqslant 10$. The minimum runtimes for both methods occur at K=10, followed by an increase in runtime for $K > 10$. This is due to the fact that when the number of available hovering positions for PD-MaxRate and MinPath-SCA exceeds the number of SNs ($N > K$), the SCA method fails to converge to a single solution. It will only reach a conclusion after reaching the maximum iterations. Finally, the proposed CSegP scheme has a significantly shorter execution time and outperforms MinPath-SCA with N=10 in terms of average data collection and SN failure rate.

3) Impact of Changes in the Average Packet Length of SNs on System Performance: We design 10 and 8 hovering positions for MinPath-SCA and PD-MaxRate, respectively. Figs. 6(a)-(b) show the effects of the average packet length of SNs, Q_{avg}^{th}, on the average data collection and the SN failure rate, respectively. First, it can be noted that as Q_{avg}^{th} grows, the average data collections of all schemes remain unchanged, while their SN failure rates increase monotonically. Second, as illustrated in Fig. 6(a), MinPath-SCA and PD-MaxRate achieve a greater average data collection with $N = 8$ compared to $N = 10$, respectively. Conversely, as depicted in Fig. 6(b), when Q_{avg}^{th}=0.5kbit, both MinPath-SCA and PD-MaxRate demonstrate elevated rates of SN failure with N= 8,

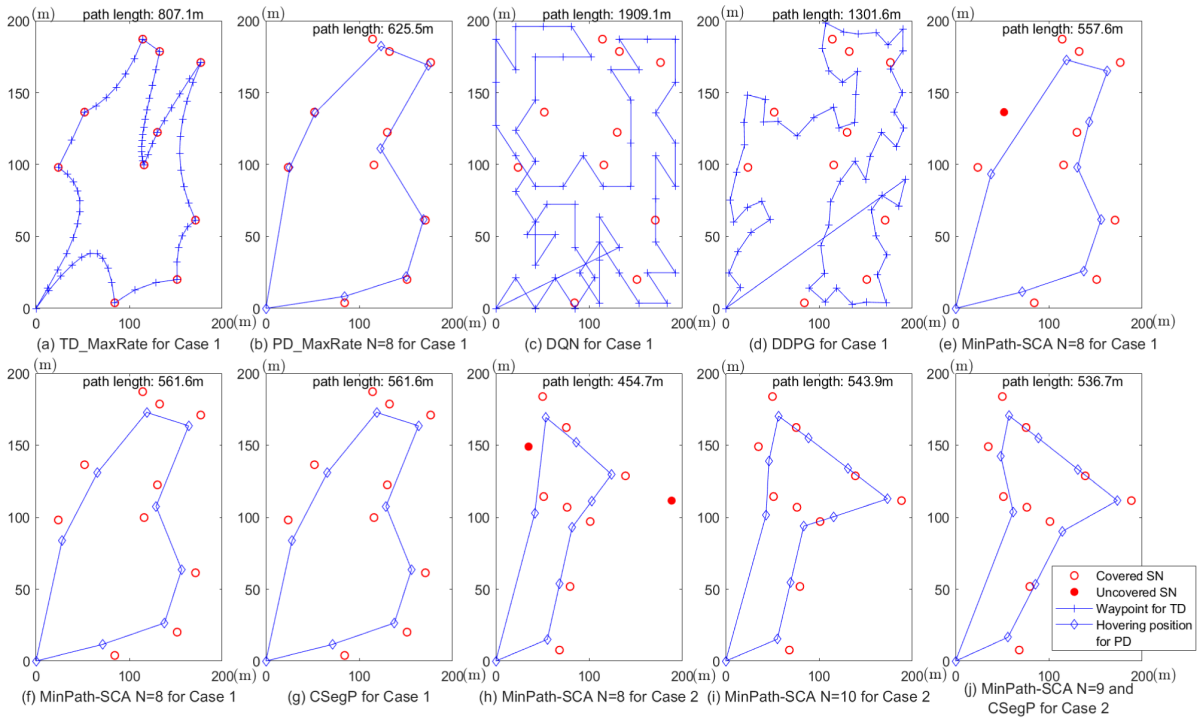

Fig. 4. Optimized UAV trajectories for 10 SNs by different schemes.

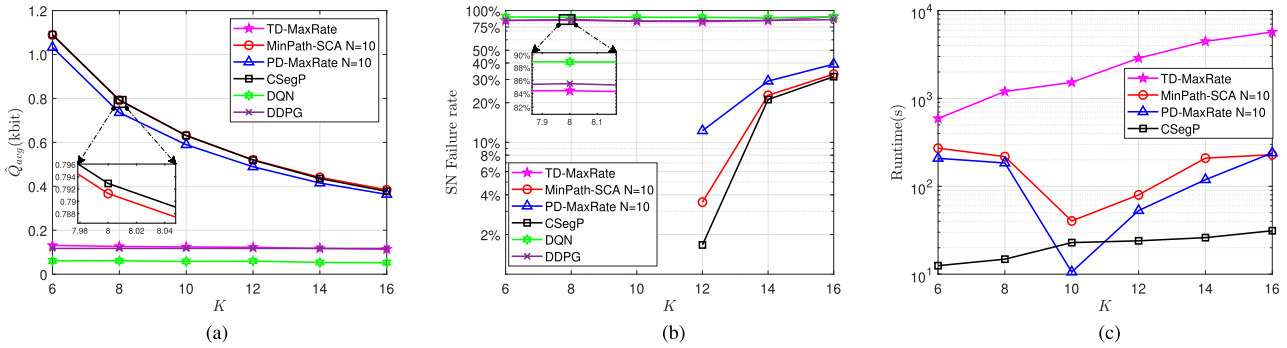

Fig. 5. (a) Average data collection versus number of SNs. (b) SN failure rate versus number of SNs. (c) Runtime versus number of SNs.

reaching 6% and 13%, respectively, while for N=10, all SNs effortlessly uploaded their data. This is due to the fact that for the PD-based trajectories, reducing the number of designable hovering points shortens the flight distance, leading to increased data collection, but some SNs may not be covered, as demonstrated in Fig. 4(h). Finally, Fig. 6 (b) demonstrates that MinPath-SCA with N=8 achieves a lower SN failure rate than both MinPath-SCA with N=10 and the proposed CSegP scheme when Q_{avg}^{th}=1kbit. The reason for this is that if the size of the information to be uploaded exceeds the maximum load of the UAV-assisted network (e.g., Q_{avg}^{th}=1kbit), some SNs may fail to upload their data, irrespective of the UAV trajectory plan. In such a scenario, employing a small number of hovering points to reduce flight distance would result in a slightly higher amount of data collected without increasing the SN failure rate. Furthermore, as Q_{avg}^{th} increases, the failure rate lines of all PD-based trajectories converge.

4) Impact of Changes in the UAV's Maximum Horizontal Coverage Radius on System Performance: To verify Lemma 1 and tell what r_{max} to set, we set $\nu = (r_{\max}/H)^2$. In addition, we design 8 and 9 hovering positions for MinPath-SCA. Figs. 7(a)-(b) show the effect of ν on the average data collection and the SN failure rate, respectively. The main observations are as follows. First, both MinPath-SCA and the proposed CSegP schemes observe an increase in the average amount of data collected with increasing ν. This is attributable to the fact that an increase in r_{max} results in a shorter UAV flight distance, allowing for more time for SNs to upload data. Second, the failure rate of SN for MinPath-SCA first decreases continuously, reaches a minimum at almost ν = 0.1, and then begins to fluctuate upwards. In contrast, for the CSegP scheme, it remains zero initially and then begins to

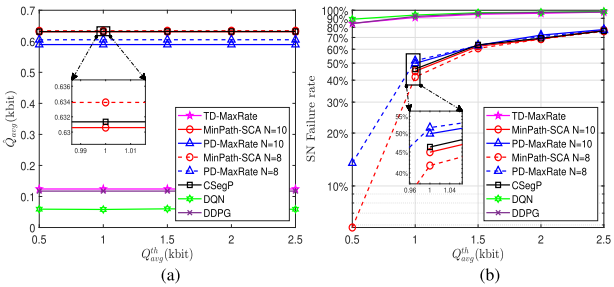

Fig. 6. (a) Average data collection versus average packet length of SNs. (b) SN failure rate versus average packet length of SNs.

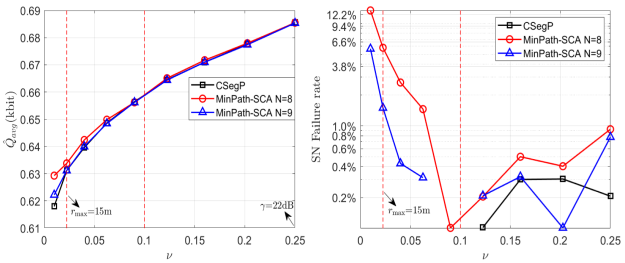

Fig. 7. (a) Average data collection versus ν. (b) SN failure rate versus ν.

fluctuate upwards similar to MinPath-SCA from almost $\nu = 0.1$. There are two main reasons for this: 1) when r_{max} is small, using only 8 or 9 hovering points in MinPath-SCA to accommodate 10 SNs can result in some SNs not being served, leading to a high failure rate. By contrast, the proposed CSegP scheme utilizes an advanced clustering algorithm based on r_{max} that effectively covers all SNs; and 2) if the condition of Lemma 1 is not satisfied, i.e., $(\frac{r_{max}}{H})^2 > 0.1$, the horizontal distances from the SNs to the UAV will begin to affect the communication links and cause the upload failures of SNs. Finally, MinPath-SCA with $N = 9$ achieves a lower SN failure rate compared to $N = 8$. However, when $\nu < 0.1$, the former shows a slightly lower average data collection than the latter. Based on the results above, it is recommended to set r_{max} to the highest value possible, as long as it satisfies the condition outlined in Lemma 1.

From the above figures, the main results are as follows. First, Figs. 4-6 demonstrates that despite the TD-based UAV trajectory schemes (e.g., TD-MaxRate) achieving a higher average SN rate than the PD-based trajectory schemes, their overall performance is inferior. For instance, the graphs in Figs. 6(a)-(b) illustrate that PD-MaxRate with $N = 10$ achieves on average 5 times higher data collection than TD-MaxRate. Additionally, when $Q_{avg}^{th} = 1$kbit, the failure rate of PD-MaxRate is only about 55% of that of TD-MaxRate. The reason for this is that in TD-based trajectories, the allocation of a fixed length of time slots to one or more SNs may fall short of completing their data uploads. Moreover, a substantial number of free time slots are left unallocated, leading to a significant waste of resources. Second, it is noticeable from Figs. 5(a)-(b) and 6(a)-(b), that for the PD-based trajectories, the schemes that minimize the UAV trajectory, including the proposed CSegP scheme and MinPath-SCA, outperform the schemes that maximize the minimum (average) achievable rate of SNs, such as PD-MaxRate. In addition, it is evident from Figs. 7(a)-(b) that the proposed CSegP scheme and MinPath-SCA attain greater average achievable data collection and lower SN failure rates at r_{max}=30m (ν=0.09) in comparison to r_{max}=15m (ν=0.0225). Therefore, our flight trajectory minimization model outperforms those depicted in Figs. 5(a)-(b) and 6(a)-(b) in terms of achievable results. Third, the number of designable hovering points affects the performance of the PD-based trajectory. For instance, setting N=8 for MinPath-SCA yields a SN failure rate of approximately 6% at Q_{avg}^{th}=0.5kbit, as depicted in Fig. 6(b). Conversely, setting N=10 for MinPath-SCA produces a reduced average data collection, as seen in Fig. 6(a). Fourth, the proposed CSegP scheme outperforms MinPath-SCA, as evidenced by the lower SN failure rate for a similar amount of data collected, as demonstrated in Figs. 5(a)-(b) and 7(a)-(b). There are two reasons for this: 1) the proposed CSegP scheme optimizes the number of hovering points based on the distribution of SNs to effectively cover all SNs with a minimal number of hovering points; and 2) for the SCA method, aside from the impact of the number of available hover points, there may be instances wherein the optimal path cannot be attained as a result of the inadequate maximum number of iterations or the random initialization of the hovering positions (refer to Fig. 4(e)). Finally, among the available options, the DRL-based frameworks including DQN and DDPG demonstrate the lowest performance. The reason is that the limited number of simulations prevents the DRL algorithm from exploring all possible paths over a large area, thus failing to obtain the optimal path.

TABLE II
CONVERGENCE ROUNDS V.S. NUMBER OF SNS AND CLUSTER SIZE

Rounds	K=8	K=10	K=12	K=14
r_{max}=15	4.28	5.06	5.08	5.17
r_{max}=25	4.58	4.83	4.95	5.36
r_{max}=35	4.39	4.76	4.83	5.43
r_{max}=45	4.48	4.08	4.03	4.58

B. Complexity and Convergence Analysis of the TSP-Based Segmented Path Optimization Scheme

In each round, K convex optimizations of path segments and a TSP with K nodes have to be solved. For the TSP, the complexity of the naive solution and the dynamic programming (DP) algorithm are $\mathcal{O}(K!)$ and $\mathcal{O}(2^K * K^2)$, respectively. The number of SNs and the cluster size, r_{max} together determine the number of iteration rounds. The detailed results of the simulation are presented in TABLE II. It is evident that the iteration rounds of the proposed optimization method are significantly lower in comparison to the SCA method's iteration complexity, $\mathcal{O}(N^{3.5}log(\frac{1}{\epsilon}))$, where $\epsilon \in [0, 1]$ is the solution accuracy [3], [33].

VII. CONCLUSION

In this research, we studied the maximum throughput for data collection from IoT devices with a deadline on each data packet in UAV-assisted networks. First, by analyzing the available resource blocks provided by UAV communication, the optimal solution for the UAV's flight trajectory is to minimize the flight distance while meeting the coverage requirements to communicate with each IoT device. To accomplish this, we proposed an advanced hierarchical clustering algorithm that guarantees coverage of all SNs with the fewest possible number of clusters. Then we developed a segmented path optimization scheme based on TSP to decompose the non-convex optimization problem of minimizing the UAV trajectory into convex subproblems. Each subproblem involves minimizing the two adjacent path segments along the trajectory. Ultimately, we transformed communication optimization into optimizing the upload time of each device in the TDMA manner. Numerical results reveal that the proposed approach drastically lowers the complexity of co-designing communication and trajectory, and achieves favorable throughput and SN failure rate performance compared to the benchmarks. Furthermore, the proposed framework is flexible for future

research in designing UAV paths for different channel models and communication forms, including non-orthogonal multiple access (NOMA), to efficiently support a large number of IoT devices.

APPENDIX
PROOF OF LEMMA 1

Assume that SN k communicates with the UAV at hovering point i. The horizontal distance between the UAV and SN k is represented by $r_{i,k} = \sqrt{(x_k - x_i)^2 + (y_k - y_i)^2}$, $0 \le r_{i,k} \le r_{\max}$ where $r_{\max}$ is the maximum horizontal coverage radius of the UAV. Therefore, equation (8) can be rewritten by

$$\hat{Q} = BT^h \frac{1}{K} \sum_{i \in \mathbf{J}} \sum_{k \in J_i} \log_2(1 + \frac{P^{\max}\beta_0}{(H^2 + r_{i,k}{}^2)\sigma^2}). \quad \text{(A-1)}$$

By extracting H^2 from the denominator of the log, we have

$$\hat{Q} = BT^h \frac{1}{K} \sum_{i \in \mathbf{J}} \sum_{k \in J_i} \log_2(1 + \frac{P^{\max}\beta_0}{H^2(1 + (\frac{r_{i,k}}{H})^2)\sigma^2}). \quad \text{(A-2)}$$

Setting $(\frac{r_{i,k}}{H})^2 \ll 1$, so we obtain

$$\hat{Q} \approx BT^h \frac{1}{K} \sum_{i \in \mathbf{J}} \sum_{k \in J_i} \log_2(1 + \frac{P^{\max}\beta_0}{H^2\sigma^2}). \quad \text{(A-3)}$$

Equation A-3 demonstrates that if the UAV meets the requirements at $(\frac{r_{i,k}}{H})^2 \ll 1$, $\forall k \in J_i$, $i \in \mathbf{J}$, the design of the UAV's flight path has minimal impact on the upload rates of data from the SNs, but has a significant impact on its hovering time and consequently on the total amount of data collected.

REFERENCES

[1] J. Liu, X. Du, J. Cui, M. Pan, and D. Wei, "Task-oriented intelligent networking architecture for the space–air–ground–aqua integrated network," *IEEE Internet Things J.*, vol. 7, no. 6, pp. 5345–5358, Jun. 2020.

[2] Y. Zeng, Q. Wu, and R. Zhang, "Accessing from the sky: A tutorial on UAV communications for 5G and beyond," *Proc. IEEE*, vol. 107, no. 12, pp. 2327–2375, Dec. 2019.

[3] Y. Guo, C. You, C. Yin, and R. Zhang, "UAV trajectory and communication co-design: Flexible path discretization and path compression," *IEEE J. Sel. Areas Commun.*, vol. 39, no. 11, pp. 3506–3523, Nov. 2021.

[4] M. Samir, S. Sharafeddine, C. M. Assi, T. M. Nguyen, and A. Ghrayeb, "UAV trajectory planning for data collection from time-constrained IoT devices," *IEEE Trans. Wireless Commun.*, vol. 19, no. 1, pp. 34–46, Jan. 2020.

[5] Y. Li, H. Zhang, K. Long, C. Jiang, and M. Guizani, "Joint resource allocation and trajectory optimization with QoS in UAV-based NOMA wireless networks," *IEEE Trans. Wireless Commun.*, vol. 20, no. 10, pp. 6343–6355, Oct. 2021.

[6] R. Ding, F. Gao, and X. S. Shen, "3D UAV trajectory design and frequency band allocation for energy-efficient and fair communication: A deep reinforcement learning approach," *IEEE Trans. Wireless Commun.*, vol. 19, no. 12, pp. 7796–7809, Dec. 2020.

[7] O. Esrafilian, H. Bayerlein, and D. Gesbert, "Model-aided deep reinforcement learning for sample-efficient UAV trajectory design in IoT networks," in *Proc. IEEE Global Commun. Conf. (GLOBECOM)*, Madrid, Spain, Dec. 2021, pp. 1–6.

[8] K. Li, W. Ni, and F. Dressler, "LSTM-characterized deep reinforcement learning for continuous flight control and resource allocation in UAV-assisted sensor network," *IEEE Internet Things J.*, vol. 9, no. 6, pp. 4179–4189, Mar. 2022.

[9] A. Benfaid, N. Adem, and B. Khalfi, "AdaptSky: A DRL based resource allocation framework in NOMA-UAV networks," in *Proc. IEEE Global Commun. Conf. (GLOBECOM)*, Madrid, Spain, Dec. 2021, pp. 1–7.

[10] T. Zhang, J. Lei, Y. Liu, C. Feng, and A. Nallanathan, "Trajectory optimization for UAV emergency communication with limited user equipment energy: A safe-DQN approach," *IEEE Trans. Green Commun. Netw.*, vol. 5, no. 3, pp. 1236–1247, Sep. 2021.

[11] Z. Sun, Z. Wei, N. Yang, and X. Zhou, "Two-tier communication for UAV-enabled massive IoT systems: Performance analysis and joint design of trajectory and resource allocation," *IEEE J. Sel. Areas Commun.*, vol. 39, no. 4, pp. 1132–1146, Apr. 2021.

[12] Y. Cui, D. Deng, C. Wang, and W. Wang, "Joint trajectory and power optimization for energy efficient UAV communication using deep reinforcement learning," in *Proc. IEEE Conf. Comput. Commun. Workshops (INFOCOM WKSHPS)*, May 2021, pp. 1–6.

[13] C. Zhan, Y. Zeng, and R. Zhang, "Energy-efficient data collection in UAV enabled wireless sensor network," *IEEE Wireless Commun. Lett.*, vol. 7, no. 3, pp. 328–331, Jun. 2018.

[14] N. Gupta, S. Agarwal, and D. Mishra, "Trajectory design for throughput maximization in UAV-assisted communication system," *IEEE Trans. Green Commun. Netw.*, vol. 5, no. 3, pp. 1319–1332, Sep. 2021.

[15] Y. Zhu and S. Wang, "Aerial data collection with coordinated UAV and truck route planning in wireless sensor network," in *Proc. IEEE Glob. Commun. Conf. (GLOBECOM)*, Dec. 2021, pp. 1–6.

[16] Y. Wang, M. Chen, C. Pan, K. Wang, and Y. Pan, "Joint optimization of UAV trajectory and sensor uploading powers for UAV-assisted data collection in wireless sensor networks," *IEEE Internet Things J.*, vol. 9, no. 13, pp. 11214–11226, Jul. 2022.

[17] B. Zhu, E. Bedeer, H. H. Nguyen, R. Barton, and J. Henry, "UAV trajectory planning in wireless sensor networks for energy consumption minimization by deep reinforcement learning," *IEEE Trans. Veh. Technol.*, vol. 70, no. 9, pp. 9540–9554, Sep. 2021.

[18] W. Du, T. Wang, H. Zhang, Y. Dong, and Y. Li, "Joint resource allocation and trajectory optimization for completion time minimization for energy-constrained UAV communications," *IEEE Trans. Veh. Technol.*, vol. 72, no. 4, pp. 4568–4579, Apr. 2023.

[19] T. Wu et al., "A novel AI-based framework for AoI-optimal trajectory planning in UAV-assisted wireless sensor networks," *IEEE Trans. Wireless Commun.*, vol. 21, no. 4, pp. 2462–2475, Apr. 2022.

[20] Q. Wu, Y. Zeng, and R. Zhang, "Joint trajectory and communication design for multi-UAV enabled wireless networks," *IEEE Trans. Wireless Commun.*, vol. 17, no. 3, pp. 2109–2121, Mar. 2018.

[21] K. Liu and J. Zheng, "UAV trajectory optimization for time-constrained data collection in UAV-enabled environmental monitoring systems," *IEEE Internet Things J.*, vol. 9, no. 23, pp. 24300–24314, Dec. 2022.

[22] Y.-Y. Guo, X.-L. Tan, Y. Gao, J. Yang, and Z.-C. Rui, "A deep reinforcement approach for energy-efficient resource assignment in cooperative NOMA-enhanced cellular networks," *IEEE Internet Things J.*, vol. 10, no. 14, pp. 12690–12702, Mar. 2023.

[23] Y.-Y. Guo, J. Yang, X.-L. Tan, and Q. Liu, "An energy-efficiency multi-relay selection and power allocation based on deep neural network for amplify-and-forward cooperative transmission," *IEEE Wireless Commun. Lett.*, vol. 11, no. 1, pp. 63–66, Jan. 2022.

[24] K. K. Nguyen, T. Q. Duong, T. Do-Duy, H. Claussen, and L. Hanzo, "3D UAV trajectory and data collection optimisation via deep reinforcement learning," *IEEE Trans. Commun.*, vol. 70, no. 4, pp. 2358–2371, Apr. 2022.

[25] B. I.-D. Ghomri, M. Y. Bendimerad, and F. T. Bendimerad, "DRL-driven optimization for energy efficiency and fairness in NOMA-UAV networks," *IEEE Commun. Lett.*, vol. 28, no. 5, pp. 1048–1052, May 2024.

[26] H. Zhang, J. Du, C. Jiang, A. Fakhreddine, A. Alhammadi, and J. Wang, "MATD3-based joint user association and resource allocation in UAV networks," in *Proc. GLOBECOM IEEE Global Commun. Conf.*, Kuala Lumpur, Malaysia, Dec. 2023, pp. 6892–6897.

[27] Z. Nazari, D. Kang, M. R. Asharif, Y. Sung, and S. Ogawa, "A new hierarchical clustering algorithm," in *Proc. Int. Conf. Intell. Informat. Biomed. Sci. (ICIIBMS)*, Okinawa, Japan, Nov. 2015, pp. 148–152.

[28] L. M. C. Cabezas, R. Izbicki, and R. B. Stern, "Hierarchical clustering: Visualization, feature importance and model selection," *Appl. Soft Comput.*, vol. 141, Jul. 2023, Art. no. 110303.

[29] L. Morissette and S. Chartier, "The k-means clustering technique: General considerations and implementation in mathematica," *Tuts. Quant. Methods Psychol.*, vol. 9, no. 1, pp. 15–24, Feb. 2013.

[30] K. Wang, J. Zhang, D. Li, X. Zhang, and T. Guo, "Adaptive affinity propagation clustering," 2008, *arXiv:0805.1096*.

[31] Y. Takashima and Y. Nakamura, "Theoretical and experimental analysis of traveling salesman walk problem," in *Proc. IEEE Asia–Pacific Conf. Circuit Syst. (APCCAS)*, Penang, Malaysia, Nov. 2021, pp. 241–244.

[32] H. P. Gavin and J. T. Scruggs, *Constrained Optimization Using Lagrange Multipliers*, document CEE 201L, Duke Univ., Durham, NC, USA, 2020.
[33] M. Razaviyayn, "Successive convex approximation: Analysis and applications," Ph.D. dissertation, Dept. Elect. Eng., Univ. Minnesota, Minneapolis, MN, USA, 2014.

Yanyan Guo received the Ph.D. degree from Beijing University of Posts and Telecommunications, Beijing, China, in 2010. She is currently an Associate Professor with the School of Physics and Electronics Engineering, Shanxi University, Taiyuan, China. Her research interests include resource allocation optimization, the Internet of Things, machine learning, and UAV networks.

Ge Xu is currently pursuing the master's degree with Shanxi University, China. She is a Graduate Student in communications engineering. Her research interests include UAV communications and artificial intelligence.

Zhicai Zhang (Member, IEEE) received the Ph.D. degree from the School of Information and Communication Engineering, Beijing University of Posts and Telecommunications, Beijing, China, in 2014. He is currently an Assistant Professor with the School of Computer Science and Technology, Hainan University, Haikou, China. From September 2017 to September 2018, he was with Carleton University, Ottawa, ON, Canada, as a Visiting Scholar. His research interests include edge intelligence, distributed machine learning, and blockchain. He received the Best Paper Award at IEEE Globecom2020. He has served as the Technical Program Committee Member for IEEE ICC'21, VTC'21 Fall, ICC'22, ICC workshop'22, and ICC'23. He serves/served as a reviewer for several journals, including IEEE JOURNAL ON SELECTED AREAS IN COMMUNICATIONS, IEEE INTERNET OF THINGS JOURNAL, IEEE TRANSACTIONS ON GREEN COMMUNICATIONS AND NETWORKING, and *IEEE Communications Magazine*.

Zengbiao Li is currently pursuing the master's degree with Shanxi University, China. He is a Graduate Student in information and communication engineering. His research interests include UAV communications and reinforcement learning.

Xinzhe You is currently pursuing the bachelor's degree with Shanxi University, China. He is a Student in the electronic information science and technology program. His research interests include UAV communications and machine learning.

Guixia Kang received the M.S. degree from Tianjin University, Tianjin, China, and the Ph.D. degree in electrical engineering from Beijing University of Posts and Telecommunications (BUPT), Beijing. She is currently a Professor with BUPT and the Director of Beijing International S and T Cooperation Base of Smart Medicine. She has expertise in the physical layer of 5G wireless systems and in the wireless e-health systems. From 2002 to 2004, she was a Research Scientist with the Future Radio Concept Department, Siemens, Munich, Germany. She is the Project Manager of several national projects, such as Important National Science and Technology Specific Project, National 863 Project, National Natural Science Foundation of China, and several international cooperation projects. She has authored one English book (Shaker Verlag, Germany), three Chinese books, and authored or co-authored over 100 journal articles and conference papers.

Lin Cai (Fellow, IEEE) received the M.A.Sc. and Ph.D. degrees in electrical and computer engineering from the University of Waterloo, Waterloo, Canada, in 2002 and 2005, respectively. Since 2005, she has been with the Department of Electrical and Computer Engineering, University of Victoria, where she is currently a Professor. Her research interests span several areas in communications and networking, with a focus on network protocol and architecture design supporting emerging multimedia traffic and the Internet of Things. She is an NSERC E.W.R. Steacie Memorial Fellow and an Engineering Institute of Canada (EIC) Fellow. In 2020, she was elected as a member of the Royal Society of Canada's College of New Scholars, Artists and Scientists; and a 2020 "Star in Computer Networking and Communications" by N2Women. She has co-founded and chaired the IEEE Victoria Section Vehicular Technology and Communications Joint Societies Chapter. She has been elected to serve the IEEE Vehicular Technology Society Board of Governors (2019–2024), and served its VP Mobile Radio in 2023. She has been a voting Board Member of IEEE Women in Engineering, from 2022 to 2023. She awarded the Outstanding Achievement in Graduate Studies. She has served as the Associate Editor-in-Chief for IEEE TRANSACTIONS ON VEHICULAR TECHNOLOGY; a member of the Steering Committee of IEEE TRANSACTIONS ON MOBILE COMPUTING, IEEE TRANSACTIONS ON BIG DATA, and IEEE TRANSACTIONS ON CLOUD COMPUTING; an Associate Editor of IEEE INTERNET OF THINGS JOURNAL, IEEE/ACM TRANSACTIONS ON NETWORKING, IEEE TRANSACTIONS ON WIRELESS COMMUNICATIONS, IEEE TRANSACTIONS ON VEHICULAR TECHNOLOGY, and IEEE TRANSACTIONS ON COMMUNICATIONS. She was the Distinguished Lecturer of the IEEE VTS Society and the IEEE Communications Society.

Laurence T. Yang (Fellow, IEEE) received the B.E. degree in computer science and technology and the B.Sc. degree in applied physics from Tsinghua University, Beijing, China, in 1992, and the Ph.D. degree in computer science from the University of Victoria, Victoria, BC, Canada, in 2006. He is a Professor with the School of Computer Science and Technology, Hainan University, Haikou, China; the School of Computer Science and Technology, Huazhong University of Science and Technology, Wuhan, China; and the Department of Computer Science, St. Francis Xavier University, Antigonish, NS, Canada. His research has been supported by the National Sciences and Engineering Research Council and the Foundation for Innovation. His research interests include parallel and distributed computing, embedded and ubiquitous computing, and big data.